Taylor & Francis
Taylor & Francis Group

Journal of Biomolecular Structure and Dynamics

ISSN: (Print) (Online) Journal homepage: www.tandfonline.com/journals/tbsd20

An *in silico* study of protein-protein interactions and design of novel peptides for TrkA in ameloblastoma

Moyim Mallick, T. R. Yoithap Prabhunath, Sonia Kumari & M. Elizabeth Sobhia

To cite this article: Moyim Mallick, T. R. Yoithap Prabhunath, Sonia Kumari & M. Elizabeth Sobhia (2024) An *in silico* study of protein-protein interactions and design of novel peptides for TrkA in ameloblastoma, Journal of Biomolecular Structure and Dynamics, 42:24, 13768-13778, DOI: 10.1080/07391102.2023.2278083

To link to this article: https://doi.org/10.1080/07391102.2023.2278083

View supplementary material

Published online: 17 Nov 2023.

Submit your article to this journal

Article views: 132

View related articles

View Crossmark data

Citing articles: 3 View citing articles

Full Terms & Conditions of access and use can be found at
https://www.tandfonline.com/action/journalInformation?journalCode=tbsd20

JOURNAL OF BIOMOLECULAR STRUCTURE AND DYNAMICS
2024, VOL. 42, NO. 24, 13768–13778
https://doi.org/10.1080/07391102.2023.2278083

Taylor & Francis
Taylor & Francis Group

Check for updates

An *in silico* study of protein-protein interactions and design of novel peptides for TrkA in ameloblastoma

Moyim Mallick[a], T. R. Yoithap Prabhunath[b], Sonia Kumari[a] and M. Elizabeth Sobhia[a]

[a]Department of Pharmacoinformatics, National Institute of Pharmaceutical Education and Research (NIPER), Sahibzada Ajit Singh Nagar, India[b]Vivekanandha Dental College for Women, Oral & Maxillofacial Pathology, Namakkal, India

Communicated by Ramaswamy H. Sarma

ABSTRACT

Ameloblastoma is a benign odontogenic jawbone tumor. The binding of Nerve growth factor (NGF) to receptor tyrosine kinase A (TrkA) promotes cell survival, proliferation, and differentiation *via* PI3K/AKT and Ras/MAPK signaling. Although the exact cause of ameloblastoma remains unknown, elevated levels of NGF and TrkA expression in ameloblastoma are associated with aggressive tumor behavior and poor patient outcomes. It is previously demonstrated that His 4, Arg 9, and Glu 11 residues of NGF made crucial interactions with the TrkA subunit. The main aim of our present study to develop potential therapeutic strategies by identifying promising peptide candidates. The objectives include starting with a detailed *in silico* analysis to identify a crucial peptide sequence of NGF that is bound by TrkA, creating a library of novel peptides from the identified peptide sequence through a single-point mutation on interacting residues (His 4, Arg 9, and Glu 11), and selecting the top peptides based on docking score, interactions analysis, and desirable pose analysis. The study ultimately designed a hybrid peptide candidate through the simultaneous and continuous mutation of the top residues, resulting in a peptide that exhibited a more specific interaction with TrkA, blocking the binding site and preventing the interaction between NGF and TrkA.

ARTICLE HISTORY
Received 11 April 2023
Accepted 26 October 2023

KEYWORDS
Nerve growth factor (NGF); tropomyosin receptor kinase A (TrkA); ameloblastoma; NGF mimetics peptides

Introduction

Ameloblastoma is a benign tumor that originates from the cells that form tooth enamel and it is unique among all benign tumors for its locally destructive and invasive nature (Brazis et al., 1995; Mendenhall et al., 2007). It is the second-most prevalent type of odontogenic tumor with microscopically different subtypes (Gardner & Corio, 1984; Masthan et al., 2015; Patsa et al., 2016). Ameloblastoma tumors are typically multicystic, with predominating follicular and plexiform histopathologic features (Hendra et al., 2020; Johnson et al., 2013; Reichart et al., 1995). It was determined that the global pooled incidence rate was 0.92 per million person-years (Hendra et al., 2020). The global sex distribution from the study of patients it is seen that 53% of patients with ameloblastoma were male and 47% were female overall, with the mandible appearing to be the favored site and a mean age of 34.3 years (Hendra et al., 2020; Reichart et al., 1995; Shear & Singh, 1978). In India, the incidence of ameloblastoma is 47.5% out of all reported odontogenic tumors and the average age was 32.5 years, Plexiform and Unicystic ameloblastoma occurred frequently (Chatterjee, n.d.; Chawla et al., 2013; Thuckanaickenpalayam Ragunathan et al., 2022). Ameloblastoma grows slowly and can be asymptomatic for years, making it difficult to diagnose in the early stages. It typically presents as a painless swelling or mass in the jaw, which can cause discomfort, difficulty chewing, and facial deformity (Attakkil et al., 2016; Mohammad et al., 2014; Palanisamy & Jenzer, 2019). Ameloblastoma's exact cause is unknown, but genetic mutations and environmental factors are thought to play a role. Presently researchers can unravel the myth behind such biologic behavior with the help of recently improved molecular techniques (Stolf et al., 2007). Treatment typically involves surgery to remove the tumor, and in some cases, radiation therapy may be necessary, however, the sort of treatment you receive will depend on the type, location, and size of your tumor as well as the cells involved (Lau & Samman, 2006).

NGF has been proven to be involved in the control of cell proliferation, survival, and differentiation in ameloblastoma cells (Aloe et al., 2015). NGF binds to distinct, high- and low-affinity cell surface receptors, p75NTR and TrkA, respectively (Mitsiadis & Pagella, 2016). NGF signaling may play regulatory functions in the proliferation and differentiation of epithelial and mesenchymal cells, according to the expression patterns of the NGF, p75NTR, and TrkA proteins during the development of human fetal teeth (Jisha et al., 2020; Micera et al., 2007; Yoithapprabhunath et al., 2020). NGF and TrkA are found in differentiated cells with secretory abilities, such as pre-and ameloblasts and odontoblasts that secrete dentine matrix and enamel matrix, respectively. However, only the proliferating cells of the dental epithelium have p75NTR

CONTACT M. Elizabeth Sobhia mesophia@niper.ac.in.

Supplemental data for this article can be accessed online at https://doi.org/10.1080/07391102.2023.2278083.

© 2023 Informa UK Limited, trading as Taylor & Francis Group

expression but do not express in these secretory cells (Mitsiadis & Pagella, 2016).

The TrkA receptor is a tyrosine kinase activated by NGF binding, and this activation triggers downstream signaling pathways that promote cell survival and proliferation. Generally, Trk receptors undergo activation in two steps: first, cell surface oligomerization of receptor molecules caused by ligands, and then, auto-phosphorylation, which means it can phosphorylate tyrosine residues on itself and other proteins. (Huang & Reichardt, 2003; Kulik & Weber, 1998; Mitsiadis & Pagella, 2016). In various cancer-causing cell, NGF binding to TrkA through phosphatidylinositol 3-kinase (PI3K)/AKT and Ras/MAPK signaling pathways enhances cell survival, proliferation, and differentiation (Huang & Reichardt, 2003).

In ameloblastoma tumors, upon NGF binding, TrkA undergoes a dimerization-induced conformational change, which activates its intrinsic kinase activity, i.e. autophosphorylation. This autophosphorylation serves as a signal for downstream signaling cascades. Phosphorylated TrkA acts as a docking site for various intracellular signaling proteins and adaptors, such as Shc and PLCγ1. Once recruited, these signaling proteins activate the intracellular PI3K/Akt pathway through Shc. Increased PI3K expression helps activate Akt and may also play a role in neoplastic alterations to the odontogenic epithelium, promoting cell survival and inhibiting apoptosis. (Amm & MacDougall, 2016; Kulik & Weber, 1998; Yuan & Cantley, 2008).

In comparison to follicular ameloblastoma, the expression level of Akt was substantially higher in plexiform ameloblastoma (Li et al., 2015). TrkA and NGF expression in ameloblastoma has been reported to be upregulated, and this has been associated with more aggressive tumor behavior and poor patient outcomes (Pagella et al., 2020). The NGF/TrkA complex is an important potential target in ameloblastoma due to its association with aggressive tumor behavior and poor outcomes. Targeting this complex can disrupt key signaling pathways involved in cell survival and proliferation. By specifically blocking the NGF/TrkA interaction, personalized therapeutic approaches can be developed to inhibit tumor growth and improve patient outcomes. Inhibiting the NGF-TrkA signaling pathway has been proposed as a potentially viable way for various cancer including ameloblastoma by inhibiting the (PI3K)/AKT signaling (Demir et al., 2016).

Hence, there is a need to inhibit the overexpression of the NGF/TrkA complex for restricting the cell proliferation of ameloblasts through the PI3K/AKT pathway. *In silico* analysis is a cost-effective and efficient approach to studying the NGF/TrkA complex in ameloblastoma. It provides a detailed understanding of atomic-level interactions and structural dynamics, aiding in targeted intervention design. Additionally, it allows for exploring various modifications and interactions, identifying novel peptide sequences, and potential therapeutic strategies.

Till now as per our knowledge, there are not that many *in silico* studies that explore the NGF/TrkA complex in ameloblastoma. The previous *in silico study* demonstrated only the important residues of NGF made crucial interaction with the TrkA subunit but the binding characteristics of the NGF/TrkA complex are not well explored in ameloblastoma and there are no *in silico* studies regarding the developing new potential therapeutic strategies or identifying promising peptide candidates that can block this complex formation to restrict the aggressive tumor growth. The main aim of our present study to develop potential therapeutic strategies by identifying promising peptide candidate.

Therefore, we intend to analyze the protein-protein interactions analysis to verify the important residues and determine the binding characteristics of the NGF/TrkA complex by molecular dynamics study, binding free energy calculations to understand the importance of interacting residues and designing novel peptides for TrkA in ameloblastoma by using relevant Computational tools such as Maestro, GROMACS, HADDOCK, and MODELLER (point mutation script) are employed for molecular interaction analysis, molecular dynamics study, docking, and peptide library design, respectively, enhancing the analytical capabilities of in silico analysis.

While we aim to address certain limitations and potential biases in our computational studies, it's important to recognize factors such as incomplete or inaccurate information about protein structures, target interactions, or compound properties, which can influence predictions. Additionally, poorly chosen parameters for molecular dynamics simulations or docking algorithms can introduce bias, and incorrect force field parameters may lead to unrealistic results. Lastly, the absence of experimental validation can render predictions speculative, while a biased interpretation of experimental results to align with computational predictions can introduce further bias. To enhance research credibility, we should acknowledge uncertainties and assumptions like simplified ligand-receptor models in computational drug design, using experiments and comparing results from various algorithms can boost research credibility and assess algorithmic uncertainties.

Materials and methods

Protein preparation of the crystal structure

For analyzing the interaction of NGF with TrkA, the RCSB Protein Data Bank (https://www.rcsb.org) was used to retrieve the protein's crystal structure (PDB ID: 1WWW) (Wiesmann et al., 1999). The structure of NGF in interaction with TrkA receptor domain 5, derived from the Homo sapiens organism, is being used here. It was obtained through X-ray diffraction with a resolution of 2.20 Å. After selecting PDB ID (1WWW), the crystal structure was imported into the Schrödinger Maestro software 2023-1, and the protein preparation wizard was used to prepare the proteins (Schrödinger, LLC, New York, NY). The Prime module of Schrödinger suite was utilized to add hydrogen atoms, and missing residues were added while water molecules beyond 5 Å from the het group of the protein crystal structure were deleted during the preprocessing step of protein preparation. For H-bond assignment, optimization was performed using the sample water orientations and the parameter PROPKA pH: 7.0. To minimize any potential steric incompatibilities in

the original PDB structures, the Impact Refinement module employs the OPLS-4e force field (Shivakumar et al., 2010) with the parameter to converge heavy atoms to RMSD 0.30 Å.

MD simulations study

MD simulations were performed on the dimer complex structure of NGF/TrkA for 100 ns by using GROMACS 2022.3 suite a Linux-based workstation (Van Der Spoel et al., 2005). CHARMM27 all-atom force field was applied and TIP3P water was used to generate the topology of the complex. The CHARMM27 all-atom force field was applied, and TIP3P water was used to generate the topology of the complex. A cubic solvation box with 51274 water molecules was employed under periodic boundary conditions, with a 10 Å distance between the box's edge and the protein's surface. To neutralize the complexes, two unit of Na + ions were added. The initial step involved energy minimization using steepest descent and conjugate gradient algorithms, with 100000 and 900000 steps, respectively, to ensure an appropriate geometry and solvent orientation in the starting structure. To achieve true dynamics, it is essential to balance the solvent and ions around the protein. Equilibration starts with NVT ensemble at 100 K for 100 ps, stabilizing at 300 K. Then, NPT ensemble is utilized with 0.1 ps coupling constants for temperature and pressure using the Berendsen algorithm.

The production phase involved a 100 ns MD simulation with a time step (dt) of 0.001 ps and a temperature of 300 K. The Nose-Hoover thermostat was used to maintain the system temperature, and the system pressure was kept at 1 bar. The cutoff for electrostatic and van der Waals interactions was set to 10 Å. Three consecutive MD runs were performed to validate and corroborate our observations and findings.

Trajectory analysis

After the MD simulations, a system stability analysis was conducted using various methods and criteria by analyzing the trajectories throughout the simulation. This included monitoring the RMSD (Root Mean Square Deviation) of the protein backbone. The range of RMSD values for stability in MD simulations may vary depending on the specific system and research context, but a commonly used threshold is around 2-3 Å. Additionally, the RMSF (Root Mean Square Fluctuation) of individual residues was analyzed. The potential energy and temperature fluctuations were also examined to ensure system equilibrium and stability throughout the simulation. Moreover, the analysis involved studying the number of hydrogen bonds within inter-chain residues of the protein-protein complex and hydrogen bond occupancy.

Binding free energy calculation

Hawk Dock server (http://cadd.zju.edu.cn/hawkdock/) was used for measuring the binding free energy of NGF interactive residues to TrkA through Generalized Born and Surface Area Solvation (MM/GB SA). It is a well-established web-based interface with efficient algorithms, including scoring functions, search algorithms, and binding site prediction, simplifies the process of performing binding free energy calculations. This is particularly advantageous when dealing with a large number of ligand-protein interactions. In the context of in silico analysis, Hawk Dock provides an additional layer of validation and refinement. The prediction of protein-protein interaction (PPI) structures involved a combination of ATTRACT docking and HawkRank re-scoring techniques. The identification of critical residues in these PPIs was accomplished through MM/GBSA free energy decomposition (Weng et al., 2019).

Designing of peptide library and molecular docking

Script for library generation

The design and generation of the peptide library using the MODELLER point mutation script involved several specific steps and criteria. Firstly, the initial peptide sequence, which serves as the reference sequence, was selected from the PDB ID: 1WWW, which has been considered as the wild-type protein-protein complex. Next, the MODELLER point mutation script was employed to introduce single point mutations in the interacting residues of the reference sequence. These interacting residues, such as His 4, Arg 9, and Glu 11, were identified as crucial for the binding of NGF with TrkA. For each mutation, the script systematically replaced the original amino acid with other possible amino acids, one at a time, generating multiple variants of the peptide sequence.

By repeating this mutation process for each interacting residue, a library of novel peptides was generated, containing different combinations of mutations at the specified positions. The peptides have been prepared after mutation before docking to remove all clashes. These steps ensured the generation of a comprehensive peptide library with variations in key interacting residues, facilitating the exploration of diverse binding characteristics and increasing the likelihood of discovering peptides with enhanced binding affinity and specificity for TrkA.

Molecular docking for the designed peptides

The peptide docking was carried out by using the high ambiguity-driven protein-protein docking (HADDOCK) server (Dominguez et al., 2003). HADDOCK is an information-driven docking program that incorporates conformational variability through ligand-protein binding site link rotations. It employs a flexible docking technique driven by encoded information from known or anticipated protein interfaces in ambiguous interaction restraints (AIRs). The docking protocol consists of three stages: randomization of orientations and rigid-body minimization (it0), semi-flexible simulated annealing in torsion angle space (it1), and refinement in Cartesian space with explicit solvent. The standard protocol generates 1000 models in the rigid body minimization stage, refining the top 200 based on energy. HADDOCK supports various experimental data types, such as NMR residual dipolar couplings, pseudo-contact shifts, and cryo-EM maps, and allows for precise distance restrictions, such as those derived from MS cross-links. It

can handle diverse modeling scenarios, including protein-protein, protein-nucleic acid, and protein-ligand complexes, including multi-body assemblies. Here in this study, the parameters used for the peptide were as follows: Clustering cutoff = 5.0 Å with the RMSD method, meaning that structures with RMSD values below 5.0 Å from each other will be grouped into the same cluster. Number of MD steps for rigid body high-temperature TAD = 2000, MD steps during the first rigid body cooling stage = 2000, MD steps during the second cooling stage with flexible side-chains at the interface = 4000, and MD steps during the third cooling stage with a fully flexible interface = 4000. The HADDOCK score is determined by the sum of van der Waals energy (EvdW), electrostatic energy (E_{elec}), desolvation energy (E_{desol}), energy from restraint violations (E_{AIR}), and the buried surface area. After simulation and water refinement, the HADDOCK score is recalculated using the formula HADDOCK score = $1.0E_{vdW} + 0.2_{Eelec} + 1.0E_{desol} + 0.1E_{AIR}$ (Spiliotopoulos et al., 2016; Vangone et al., 2017).

Result and discussion

Structure details of NGF/TrkA complex

The 3D structure of NGF in interaction with TrkA receptor domain 5 was reported by Wiesmann et al. (Figure 1). TrkA is a tyrosine kinase-active receptor that creates a highly specific binding site for NGF. The TrkA-d5 domain is needed and adequate for NGF binding. The crystal structure is a homodimer of NGF and TrkA 2:2 subunit. The NGF subunits contain two identical chains named chain W and chain V each of them containing 120 amino acids, with residue numbers ranging from 1 to 120 in the PDB structure, on the other hand, TrkA subunits also contain two identical chains named chain X and chain Y, each of them containing 101 amino acids, with residue numbers ranging from 282 to 382 in the PDB structure.

The crystal structure reveals two protein-protein interaction patches: the 'first patch' and the 'second patch'. The first patch involves NGF residues (β strand bundle) interacting with the loops (loop1 containing residues 30-35) at the C-terminal end of Trk-d5. Due to the conservation of these residues among all neurotrophins, this contact is known as the 'conserved patch'.

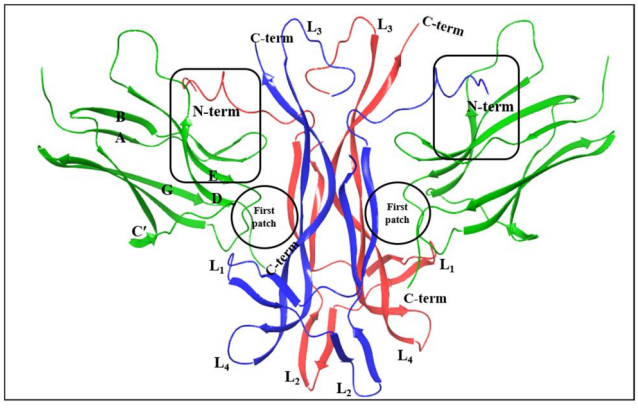

Figure 1. Overall three-dimensional structure of NGF in interaction with domain 5 of the TrkA receptor (NGF subunits in red and blue colour while TrkA subunits are in green colour).

On the other hand, the second patch consists of the N-terminus (residues 2-13) of NGF interacting with the ABED β sheet of the TrkA subunit. This 'second patch' is crucial for the specificity of NGF binding to TrkA and distinguishes NGF from other neurotrophins. As a result, it is also referred to as the 'specific patch'.

In this current study, the exclusive focus is on the analysis and investigation of the second patch (specific patch).

Interaction analysis of vital residues at the protein-protein interface

After the overall discussion of the NGF/TrkA complex structure, the protein preparation was done, and missing residues and hydrogen atoms were added using Prime module. The 'specific patch' was analyzed as it contains the N-terminal fragment of NGF, previously demonstrated to be responsible for high-affinity binding with TrkA. During the protein-protein interaction analysis of the NGF and TrkA complex, it was observed that similar interactions are present between chains W/X and chains V/Y in the 'specific patch', possibly due to their homodimeric nature (NGF and TrkA 2:2 subunit). The vital residues of NGF interacting with TrkA in the 'specific patch' (ABED β sheet of TrkA) are His 4, Arg 9, and Glu 11 from chain W, and Phe 303, His 297, Glu 334, Arg 347, and His 353 from chain X of the TrkA subunit (Figure 2).

This present study on protein-protein interactions has identified significant findings on the binding mechanism between the NGF and TrkA subunits. Previous research (Berrera et al., 2006; Wiesmann et al., 1999) has established the critical role played by His 4, Arg 9, and Glu 11 residues of chain W in the NGF subunit. However, our study has explored additional important interactions within a 'specific patch' that had not been previously explored. Specifically, we have observed a salt bridge between Arg 347 and Glu 11, as well as pi-stacking interactions involving His 4 with His 343 and His 291. These interactions underscore the significance of the His 4 and Glu 11 residues of the NGF subunit in binding with the TrkA subunit, while also highlighting the importance of residues His 291 and His 343 in this interaction. The residues of the NGF subunit present at the 'specific patch' are unique for the NGF/TrkA complex, whereas the residues and interactions present at the 'conserved patch' are the same for the complex of NGF with other TrK subfamily members (TrkB/TrkC). Therefore, these identified residues of NGF and interactions with TrkA contribute to understanding the NGF/TrkA complex. Our findings provide new insights for researchers seeking to identify critical interacting residues of the TrkA subunit on the 'specific patch' that interact with the NGF subunit.

Molecular dynamics

Molecular dynamics study helped us to understand the binding characteristics of the NGF/TrkA complex through the various types of analysis like rmsd, rmsf, and h-bond analysis

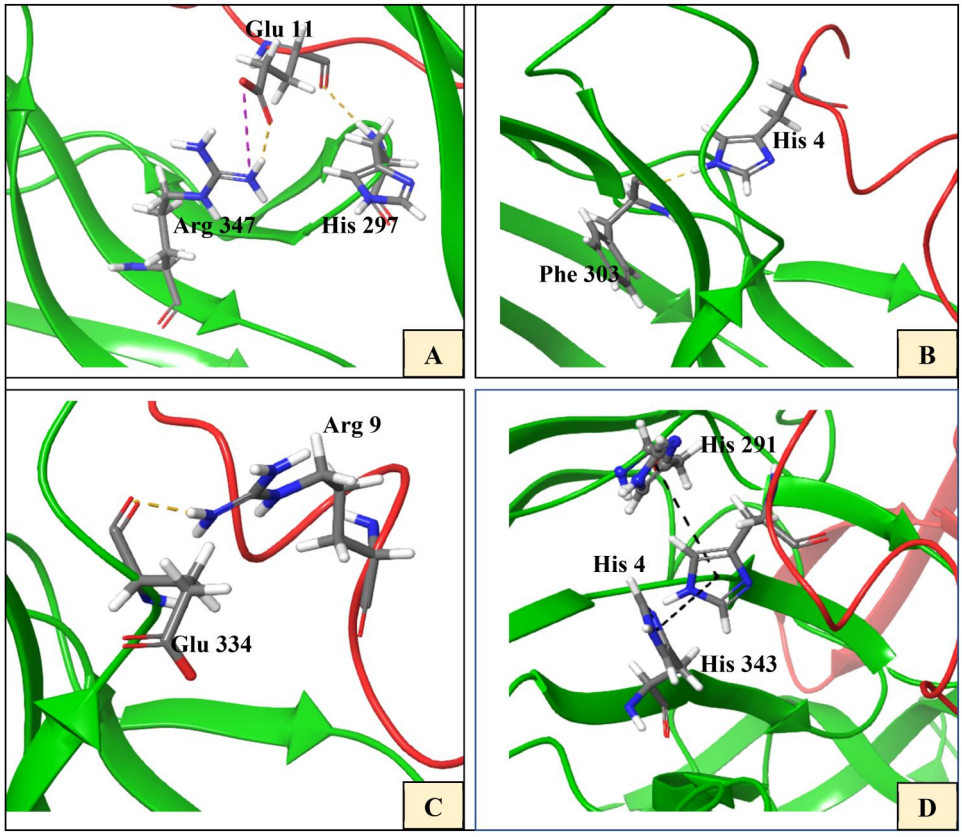

Figure 2. (A). Two hydrogen bonds interaction with Glu 11 between His 297, Arg 347, salt bridge (purple) between Arg 347 and Glu11, (B). hydrogen bonding interactions His 4 with Phe 303 (C). hydrogen bonding between Arg 9 and (D). pi stacking interactions (black) His 4 with His 343 and His 291.

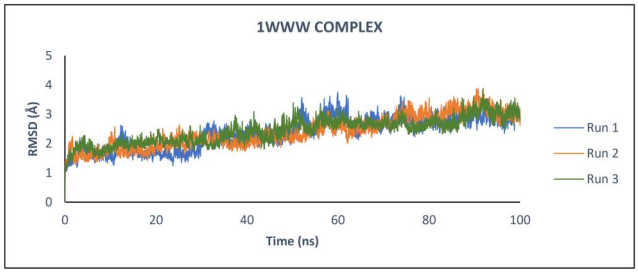

Figure 3. RMSD results of triplicate MD simulations of NGF/TrkA complex. Run 1(blue) i.e. for the first MD study, average RMSD value was 2.37 Å. Run 2(orange) i.e. for the second time MD study, average RMSD value was 2.39 Å. Run 3(green) i.e. for the third time MD study, average value was 2.40 Å.

followed by binding energy calculation. Our intention of md is to investigate the stability of the whole complex and analyze the 'specific patch' only rather than the MD analysis of the whole NGF-TrkA domain 5 Complex (Settanni et al., 2003) because domain 5 contains two units of NGF and two units of TrkA and it has different interacting region but for our present study, we have focused on only 'specific patch' as it was previously demonstrated to be an important determinant for affinity and specificity in the binding to trkA (Wiesmann et al., 1999).

RMSD analysis

The stability of the whole protein-protein complex was evaluated through rmsd analysis by using MD simulation for 100 ns in triplicate (Figure 3). According to the analysis, it was observed that the entire complex exhibited some mobility in the presence of a solvent, mainly due to the more mobile nature of the TrkA subunit. It was also observed that in the case of Run 1, i.e. the first MD study, the complex stabilized after 50 ns, and from 60 ns to 100 ns, the complex remained consistently stable, with an average RMSD value of 2.37 Å. In contrast, in Run 2 and Run 3, the complex remained sufficiently stable throughout the simulation, with average RMSD values of 2.39 and 2.40 Å, respectively.

RMSF analysis

Like RMSD in terms of numerical measurement, RMSF (root mean square fluctuation) quantifies differences in positions between individual structures over time. RMSF measures the flexibility of each residue, or how much it moves or fluctuates throughout a simulation. Like the protein-protein interaction analysis, analogous fluctuations have been observed here between each subunit of NGF (specifically, chains W and V) and TrkA (specifically, chains X and Y). Consequently, in this context, the RMSF for only one unit of NGF and TrkA is presented. The average RMSF value for the NGF subunit was 1.29, 1.38, and 1.40 Å for the triplicate MD (Figure 4A), respectively. In contrast, the average RMSF value of the TrkA subunit was 1.65, 1.75, and 1.78 Å for the triplicate MD study (Figure 4B). These values indicate that the TrkA subunit is more mobile than the NGF subunit in plasma protein.

Here, the 'specific patch' has been analyzed, and for a better understanding, the average RMSF for the triplicate MD

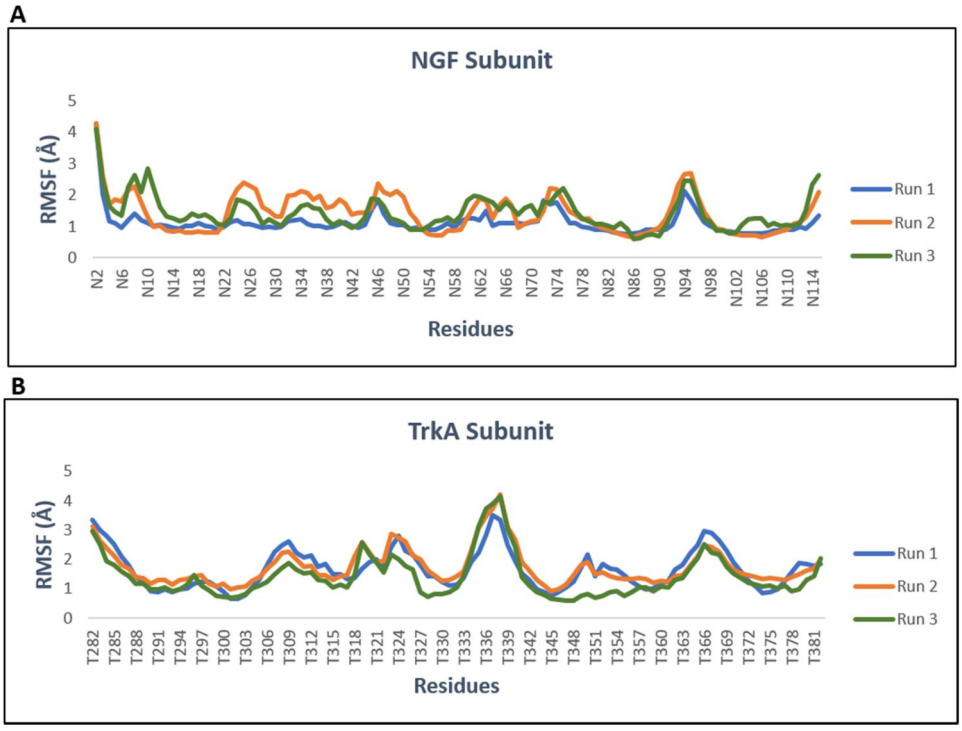

FIGURE 4. *A) RMSF results of triplicate MD simulations of NGF subunit. Run 1(blue)* i.e. *for the first time MD study, average RMSF value was 1.29 Å. Run 2(orange)* i.e. *for the second time MD study, average RMSF value was 1.38 Å. Run 3(green)* i.e. *for the third time RMSF value was 1.40 Å. B) RMSF results of triplicate MD simulations of TrkA subunit. Run 1(blue)* i.e. *for the first time MD study, average RMSF value was 1.65 Å. Run 2(orange)* i.e. *for the second time MD study, average RMSF value was 1.75 Å. Run 3(green)* i.e. *for the third time RMSF value was 1.78 Å. (N-NGF residues, T-TrkA residues).*

study was calculated for the residues His 4 (1.179 Å), Arg 9 (1.189 Å), and Glu 11 (1.007 Å) in the NGF subunit, which interact with residues Phe 303 (0.801 Å), Glu 334 (1.975 Å), and Arg 347 (1.157 Å) in the TrkA subunit. This indicates that the interacting residues are binding with no remarkable fluctuation on the specific patch.

Hydrogen bond analysis

The quantity of hydrogen bonds in a system of interest is determined through hydrogen bond analysis. A hydrogen bond is created when two heavy atoms share a hydrogen atom (H). It is joined by covalent bonds to both the 'donor' and the 'acceptor', which are both heavy atoms (Sodeifian & Razmimanesh, 2019). The binding strength between NGF/TrkA protein-protein complex might be assessed with the help of intermolecular hydrogen bonds. In this analysis, the total number of donor atoms for triplicate MD study was 611, 623, and 630, and the total number of acceptor atoms was 1180, 1191, and 1201 at the protein-protein interfaces. The hydrogen bond analysis shows that one hydrogen bond remains constant until 100 ns, and the maximum number of hydrogen bonds formed is four throughout the simulation (Figure 5).

The hydrogen bond occupancy has been examined and it was found that the average occupancy between Arg 9-Side chain and Glu 334-Side chain was 97.75%, 81.70% was between Arg 347-Side chain and Glu 11-Side chain, 55.13% in between His 297-Main chain and Glu 11-Main chain, 69.80% in between Phe 12-Main chain and Leu 112-Main chain, 93.28% in between Arg 69-Side chain and Ser 13-Main chain and 59.34% in between His 4-Side chain and Phe 303-Main chain. The hydrogen bond occupancy percentages provide information about the number of trajectories that participated in hydrogen bond formation during a simulation.

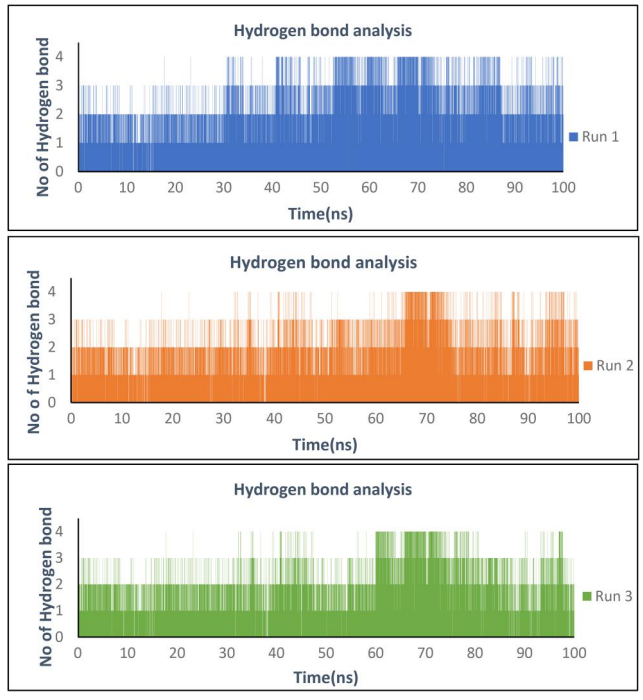

Figure 5. Hydrogen bond result of triplicate MD simulations of NGF/TrkA complex, 1 hydrogen bond is constant till 100 ns and the maximum number of hydrogen bonds formed is 4 throughout the simulation for Run 1(blue) i.e. for the first time MD study, Run 2(orange) i.e. for the second time MD study. Run 3(green) i.e. for the third time MD study.

Specifically, the residues His 4, Arg 9, Glu 11, Phe 12, and Ser 13 of the 'specific patch' were found to have significant occupancy in hydrogen bond interactions with the TrkA subunit. This suggests that these residues may play a key role in the interaction between the NGF and TrkA subunit. Overall, the analysis of hydrogen bond interactions can provide insight into the specific residues and patches that are involved in molecular interactions.

Binding-free energy analysis

In the present study, the binding free energy calculations were used to determine the importance of specific residues in the binding of NGF with the TrkA subunit. In the binding free energy calculation of the 'specific region' (residue 2 to 13) of the NGF/TrkA subunit (Figure 6), it was seen that the total binding energy of His 4 was −5.15 kcal/mol and Ile 6 was −4.72 kcal/mol and Arg 9 has the highest electrostatic energy −60.12 kcal/mol and the total binding energy of Glu 11 also has −4.21 kcal/mol. Here the total energy is the summation of van der Waals (VDW), electrostatic (ELE), generalized Born (GB), and surface area (SA) contribution. The more negative binding energy indicates that more energy is formed in the bound state than the unbound state of the residue so, the residue that shows total energy negative is important for binding characteristics. The complete binding free energy for all the residues on the 'specific region' are given in Supportive material Table S1.

From the binding free energy calculation (Supportive material Table S1), it is evident that the residues His 4, Pro 5, Ile 6, Phe 7, Arg 9, Gly 10, Glu 11, Phe 12, and Ser 13 exhibit negative total binding free energy, indicating their significance in the binding process. Conversely, residues Ser 2, Ser 3, and His 8 display positive binding free energy, suggesting their lesser importance in binding. This data aids in identifying potential residues crucial for the binding of NGF with the TrkA subunit in the 'specific patch'. Overall, binding free energy calculations provide valuable insights into specific residues essential for molecular interactions.

Our study began with an analysis of the protein-protein interactions in the NGF/TrkA complex, revealing the involvement of residues His 4, Arg 9, and Glu 11 in these interactions. Molecular dynamics simulation was then conducted to assess the complex's stability, which showed sufficient stability with minimal rmsf fluctuations. Hydrogen bond analysis highlighted the significance of residues His 4, Arg 9, Glu 11, Phe 12, and Ser 13 throughout the simulation. Additionally, binding free energy calculations indicated the importance of residues His 4, Pro 5, Ile 6, Phe 7, Arg 9, Gly 10, Glu 11, Phe 12, and Ser 13 for NGF's binding to the TrkA subunit. Through comprehensive analysis and discussions, the sequence H4PIFHRGEFS13 was identified as a key player in the binding of NGF with the TrkA subunit in the 'specific patch'.

Overall, the study provides valuable insights into the importance of identified NGF residues and molecular interactions involved with TrkA at the 'specific patch' that helps to understand the contribution to our understanding of the NGF/TrkA complex and also describes the successful identification of the protein sequence of NGF subunit that can be targeted as a reference for designing novel peptides for TrkA in ameloblastoma.

The findings have potential applications in drug development and therapeutic interventions. By targeting the identified residues or disrupting the crucial interactions, it may be possible to modulate the NGF/TrkA signaling pathway. This could lead to the development of novel drugs or therapeutic strategies aimed at inhibiting or modulating the activity of the NGF/TrkA complex. Such interventions may have implications in the treatment of conditions where aberrant NGF/TrkA signaling is involved, including ameloblastoma and other related diseases.

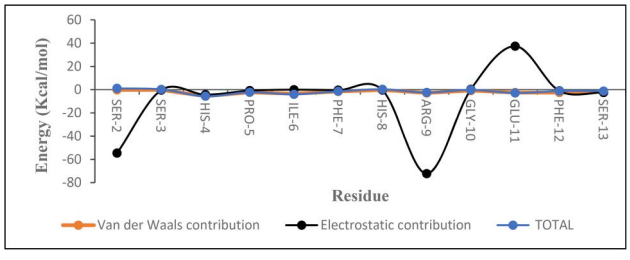

Figure 6. Binding free energy calculation of NGF residues interacting with TrkA on the specific region (highlighting van der Waals, electrostatic contribution, and total energy. the total binding energy of His 4 was -5.15 kcal/mol and Ile 6 was -4.72 kcal/mol and Arg 9 has the highest electrostatic energy -60.12 kcal/mol and the total binding energy of Glu 11 also has -4.21 kcal/mol.

Designing of peptide library

The peptide library construction involved the use of the protein sequence H4PIFHRGEFS13 as the reference peptide sequence, derived from the monomer structure of NGF/TrkA. This sequence is essential for the binding of NGF with TrkA. The choice to exclusively employ the monomer structure was informed by prior observations in protein-protein interaction analysis and MD studies, which confirmed the presence of analogous interactions and binding characteristics in both monomers. The residue His 4, Arg 9, and Glu 11 were mutated by a single point mutation at a time with the remaining amino acids to design a library of 57 novel peptides. To create a hybrid peptide, the residue His 4, Arg 9, and Glu 11 residues were altered simultaneously, and a single-point mutation by the amino acid that is selected for the above position during single-point mutation. The exhaustive list of the top 4 peptide sequences, filtered out based on docking score, pose, and interaction analysis during further study, is shown in Table 1. All these alterations are highlighted in red.

Table 1. The top four peptides by single point mutation and the hybrid peptide by simultaneous mutation (red marks are used to identify mutant residues).

Mutated peptide	Sequences of peptide
Reference peptide	H4PIFHRGEFS13
1	D4PIFHRGEFS13
2	HPIFHK9GEFS13
3	HPIFHRGD11FS13
4 (Hybrid peptide)	D4PIFHK9GD11FS13

Molecular docking and interaction analysis

The active site of the TrkA receptor was docked with all 57 of the proposed peptides and reference peptides. The TrkA receptor residues 291, 297, 303, 334, 343, and 347 were chosen as active site residues because they were directly involved in the interaction with NGF subunits. The greatest docking poses with the highest negative HADDOCK ratings were filtered out. The docking scores of all 57 peptides are given in Supportive material Table S2. Figure 7, describes the process of generating a hybrid peptide using favorable mutation analysis and sorting out the best peptide based on docking score and pose and interactions analysis. A library of 57 peptides was taken, and the best peptides were selected for each of the mutated positions (4, 9, and 11), as represented in the mutation analysis wheel. From the favorable mutation analysis, the top 3 peptides were sorted out for each of the above-mentioned positions, and finally, a hybrid peptide was designed by simultaneous and single point mutation using the best selected amino acids from the identified positions (4,9, and 11). Overall, this process involves selecting the best peptides based on docking score, pose, and interactions analysis and combining them to generate a hybrid peptide with improved binding properties. The docking score of the reference peptide was −72.5 ± 1.0 Kcal/mol whereas the top three screened peptides were −72.2 ± 1.8 Kcal/mol, −78.3 ± 3.2 Kcal/mol, and −81.4 ± 3.6 Kcal/mol. The docking score of the hybrid peptide was −76.0 ± 1.5 Kcal/mol and there were more interactions with the active site of the TrkA receptor.

The information presented in Figure 7, displays the amino acid sequences, docking scores, and hydrogen bond interactions of the best-screened 4 mutated peptides (including a hybrid peptide) generated from the reference peptide sequence. The designed peptide is also shown, with the mutated residue marked in magenta color (Figure 8). The interactions of the reference peptide (Wild type, **H4PIFHRGEFS13**) were 6 hydrogen bonds with His 297, Phe 303, Glu 334 (2), and Arg 347 (2), 1 Pi stacking with His 343, and 1 salt bridge with Arg 347, **1.** mutated at residue 4 (**D4PIFHRGEFS**) were 6 hydrogen bons with His 297, Phe 303, Glu 334 (2), Arg 347 (2), 1 Pi stacking with His 291 and 1 Salt bridge with Arg 347, **2.** mutated at residue 9 (**HPIFHK9GEFS**) were 5 hydrogen bonds with His 297, Phe 303, Glu 224, Arg 347 (2), 1 Pi stacking with His 343, 2 Salt bridge with Glu 334, Arg 347, **3.** mutated at residue 11 (**HPIFHRGD11FS**) were 6 hydrogen bonds with Met 296, His 297, Phe 303, Glu 334, Arg 347 (2), 2 Pi stacking His 291, His 343, 2 Salt bridge with Glu 334, Arg 347, whereas the hybrid peptide (Simultaneous mutation at residue 4, 9, and 11, D4PIFHK9GD11FS) has more interactions than the reference peptide.

The interactions of the hybrid peptide (D4PIFHK9GD11FS) with the TrkA receptor, as shown in Figure 9. The figure demonstrates that the residue ASP 4 of the hybrid peptide formed two hydrogen bonds with His 291 and Ser 304, while Lys 9 formed two hydrogen bonds and one salt bridge with Glu 334. Asp 11 made one hydrogen bond with His 297 and two hydrogen bonds and one salt bridge with Arg 347, and Ser 13 formed one hydrogen bond with Met 296. The figure shows that the hybrid peptide made more interactions compared to other peptides, such as D4PIFHRGEFS, HPIFHK9GEFS, and HPIFHRGD11FS. Overall, the hybrid peptide showed improved interactions with the TrkA receptor, potentially leading to improved binding properties.

The binding free energy calculation revealed that residues 4, 5, 6, 7, 9, 11, 12, and 13 had negative binding energy, indicating their potential for creating interactions with the receptor during binding. After mutation, residue 13 was found to have created additional interactions with the TrkA subunit while retaining the wild-type interactions, resulting in a stronger peptide that can block the TrkA binding site. This study demonstrated the importance of the residue sequence H4PIFHRGEFS13 for designing novel peptides by mutation whereas a previous study (Berrera et al., 2006)

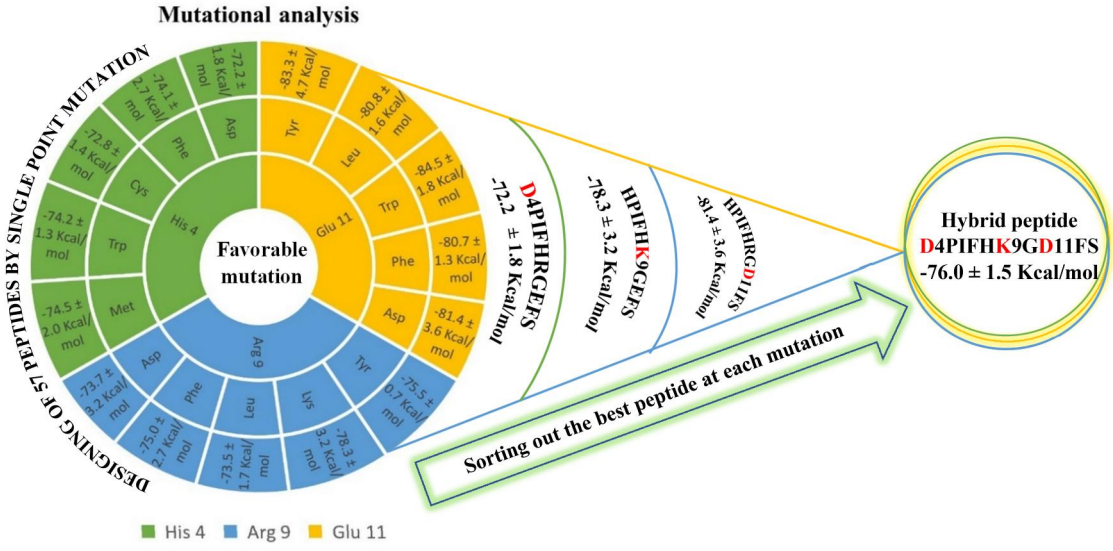

Figure 7. The favorable mutation analysis involves sorting out the best peptide by considering docking score and pose. The strategy began with a total of 57 peptides. Based on the selection criteria, the top 3 peptides were chosen for each mutated position, and finally, a hybrid peptide was generated.

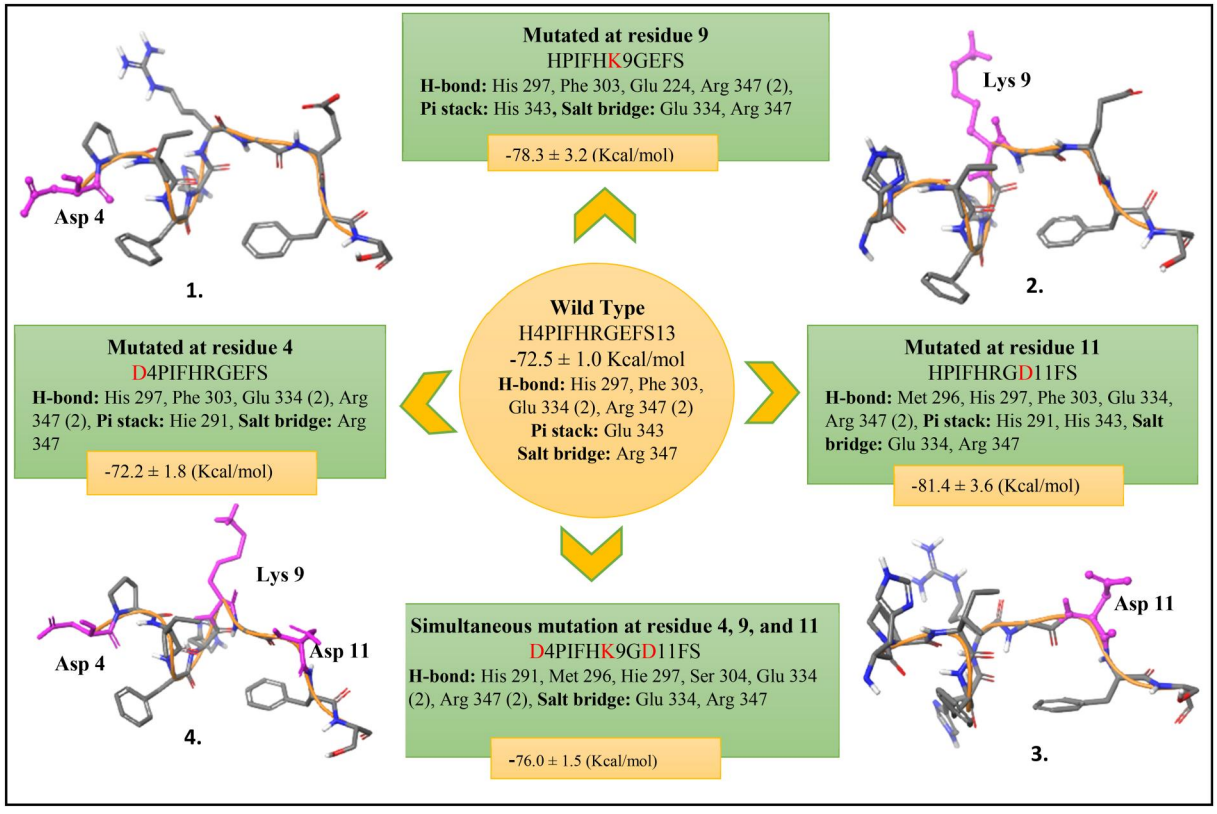

Figure 8. Amino acid sequences, docking scores, and hydrogen bonds, pi-stack, salt bridge interactions of the four best-screened mutated peptides (magenta colour representing the mutated residue) are compared to the wild-type peptide in the Middle of the representation.

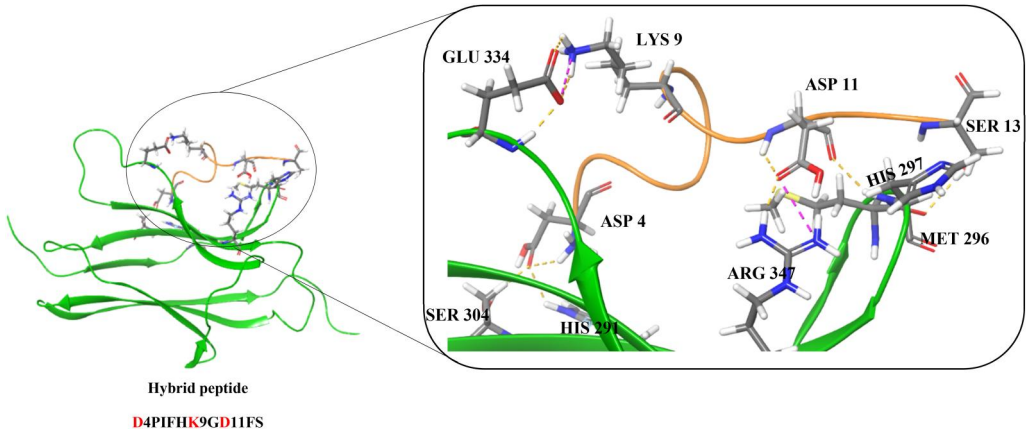

Figure 9. Different type of interactions of hybrid peptide (orange) with the TrkA receptor (green) (for clarity, interacting residues are marked in the inset).

uncovered that the wild-type $_{ACE}$HPIFGRGEF$_{NME}$ peptide may provide high affinity to the trkA-d5 receptor.

MD simulation study for designed peptide

RMSD

MD simulation was performed for 100 ns to assess the stability of the best-designed hybrid protein-peptide complex with the wild-type protein-peptide complex. According to this analysis, it is observed that the designed protein-peptide complex gained more stability than the wild-type protein-peptide complex throughout the simulation. The average RMSD value for the wild type is 2.238, 2.512, and 2.871 Å (Figure 10) for the triplicate MD study, whereas the RMSD value of the hybrid protein-peptide complex was 2.220, 2.864, and 2.506 Å (Figure 11). The hybrid protein-peptide complex showed no significant fluctuations compared to the wild type.

RMSF

The root-mean-square fluctuation (RMSF) is a measure of the average deviation of the position of each atom in a protein or other molecular structure from its average position over the course of a simulation. The average RMSF value for the wild type peptide was 2.64, 1.98, and 3.07 Å for the triplicate MD, respectively (Figure 12). In contrast, the average RMSF value of the hybrid peptide was 2.64, 1.95, and 3.05 Å for the

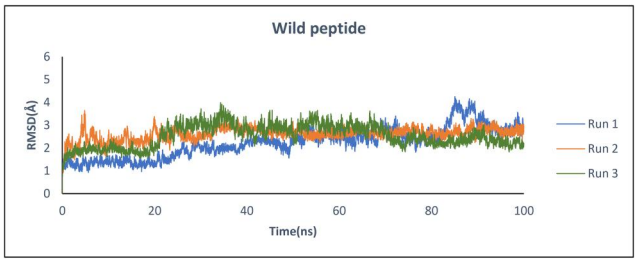

Figure 10. RMSD results of triplicate MD simulations of wild peptide. Run 1(blue) i.e. for the first time MD study, average RMSD value was 2.238 Å. Run 2(orange) i.e. for the second time MD study, average RMSD value was 2.512 Å. Run 3(green) i.e. for the third time RMSD value was 2.871 Å.

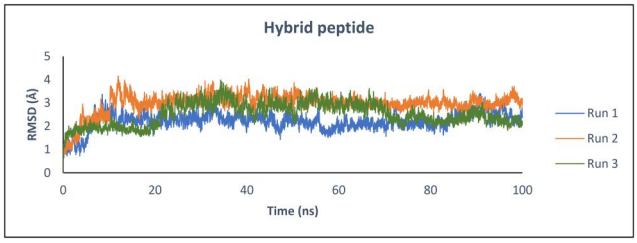

Figure 11. RMSD results of triplicate MD simulations of hybrid peptide. Run 1(blue) i.e. for the first time MD study, average RMSD value was 2.220 Å. Run 2(orange) i.e. for the second time MD study, average RMSD value was 2.864 Å. Run 3(green) i.e. for the third time RMSD value was 2.506 Å.

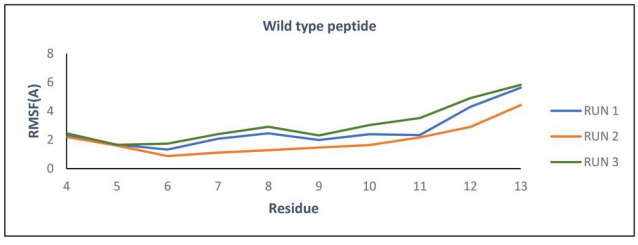

Figure 12. RMSF results of triplicate MD simulations of *WILD PEPTIDE*. Run 1(blue) i.e. for the first time MD study, average RMSF value was 2.64 Å. Run 2(orange) i.e. for the second time MD study, average RMSF value was 1.98 Å. Run 3(green) i.e. for the third time value was 3.07.

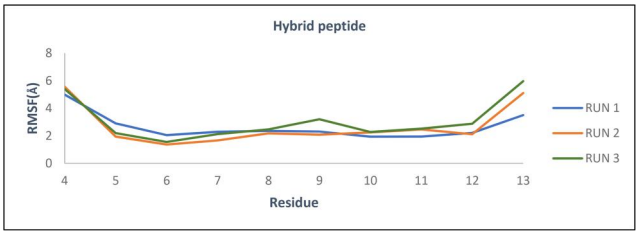

Figure 13. RMSF results of triplicate MD simulations of hybrid peptide. Run 1(blue) i.e. for the first time MD study, average RMSF value was 2.64 Å. Run 2(orange) i.e. for the second time MD study, average RMSF value was 1.95 Å. Run 3(green) i.e. for the third time value was 3.04.

triplicate MD study (Figure 13). In this analysis, it is observed that the hybrid peptide residues have lower fluctuation compared to the wild type from residues 10 to 13.

Conclusion

This study aimed to identify the crucial peptide sequence of the NGF subunit responsible for interacting with the TrkA subunit and to design novel NGF mimetic peptides for reducing TrkA receptor overexpression. Through comprehensive analysis and discussions, including interaction analysis, MD simulation, and binding free energy calculations, the sequence H4PIFHRGEFS13 was identified as playing a key role in the binding of NGF with the TrkA subunit in the 'specific patch'. A library of 57 new peptides was designed by single-point mutation of these residues, and the top three peptides were selected based on docking and interaction studies. The study ultimately designed a hybrid peptide (D4PIFHK9GEFD13) by simultaneously and singly mutating the top three residues. This hybrid peptide, with more specific interactions than the reference peptide can effectively bind and block TrkA binding site, thereby inhibiting the interaction between NGF and TrkA on the 'specific patch'.

Disclosure statement

No potential conflict of interest was reported by the authors.

Funding

The author(s) reported there is no funding associated with the work featured in this article.

References

Aloe, L., Luisa Rocco, M., Omar Balzamino, B., & Micera, A. (2015). Nerve growth factor: A focus on neuroscience and therapy. *Current Neuropharmacology*, *13*(3), 294–303. https://doi.org/10.2174/1570159X13666150403231920

Amm, H. M., & MacDougall, M. (2016). Molecular signaling in benign odontogenic neoplasia pathogenesis. *Current Oral Health Reports*, *3*(2), 82–92. https://doi.org/10.1007/s40496-016-0085-z

Attakkil, A., Thorawade, V., Kar, R., Chandran, S., Rengaraja, D., Rao, K., & Rohe, D. (2016). Large ameloblastoma of mandible: Our experience with intermaxillary fixation. *International Journal of Otolaryngology and Head & Neck Surgery*, *05*(01), 17–22. https://doi.org/10.4236/ijohns.2016.51003

Berrera, M., Cattaneo, A., & Carloni, P. (2006). Molecular simulation of the binding of nerve growth factor peptide mimics to the receptor tyrosine kinase A. *Biophysical Journal*, *91*(6), 2063–2071. https://doi.org/10.1529/biophysj.106.083519

Brazis, P. W., Miller, N. R., Lee, A. G., & Holliday, M. J. (1995). Neuro-ophthalmologic aspects of ameloblastoma. *Skull Base Surgery*, *5*(4), 233–244. https://doi.org/10.1055/s-2008-1058921

Chatterjee, S. (n.d.). *A 10-year prevalence study of solid ameloblastomas, unicystic ameloblastomas, and ameloblastic carcinoma in a North Indian population subset.*

Chawla, R., Ramalingam, K., Sarkar, A., & Muddiah, S. (2013). Ninety-one cases of ameloblastoma in an Indian population: A comprehensive review. *Journal of Natural Science, Biology and Medicine*, *4*(2), 310. https://doi.org/10.4103/0976-9668.116984

Demir, I. E., Tieftrunk, E., Schorn, S., Friess, H., & Ceyhan, G. O. (2016). Nerve growth factor & TrkA as novel therapeutic targets in cancer. *Biochimica et Biophysica Acta*, *1866*(1), 37–50. https://doi.org/10.1016/j.bbcan.2016.05.003

Dominguez, C., Boelens, R., & Bonvin, A. M. J. J. (2003). HADDOCK: A protein-protein docking approach based on biochemical or biophysical information. *Journal of the American Chemical Society*, *125*(7), 1731–1737. https://doi.org/10.1021/ja026939x

Gardner, D. G., & Corio, R. L. (1984). Plexiform unicystic ameloblastoma: A variant of ameloblastoma with a low-recurrence rate after enucleation. *Cancer*, *53*(8), 1730–1735. https://doi.org/10.1002/1097-0142(19840415)53:8%3C1730::AID-CNCR2820530819%3E3.0.CO;2-U

Hendra, F. N., Van Cann, E. M., Helder, M. N., Ruslin, M., de Visscher, J. G., Forouzanfar, T., & de Vet, H. C. W. (2020). Global incidence and profile of ameloblastoma: A systematic review and meta-analysis. *Oral Diseases*, *26*(1), 12–21. https://doi.org/10.1111/odi.13031

Huang, E. J., & Reichardt, L. F. (2003). Trk receptors: Roles in neuronal signal transduction. *Annual Review of Biochemistry*, *72*(1), 609–642. https://doi.org/10.1146/annurev.biochem.72.121801.161629

Jisha, G. B., Ilayaraja, V., Yoithapprabhunath, T. R., Ganapathy, N., Dineshshankar, J., & Nirmal, R. M. (2020). Immunohistochemical detection of Tyrosine Kinase receptor (TrK) in follicular and plexiform ameloblastoma–A novel study. *Journal of Oral and Maxillofacial Pathology: JOMFP*, *24*(1), 125–130. https://doi.org/10.4103/jomfp.JOMFP_220_19

Johnson, N. R., Savage, N. W., Kazoullis, S., & Batstone, M. D. (2013). A prospective epidemiological study for odontogenic and non-odontogenic lesions of the maxilla and mandible in Queensland. *Oral Surgery, Oral Medicine, Oral Pathology and Oral Radiology*, *115*(4), 515–522. https://doi.org/10.1016/j.oooo.2013.01.016

Kulik, G., & Weber, M. J. (1998). Akt-dependent and-independent survival signaling pathways utilized by insulin-like growth factor I. *Molecular and Cellular Biology*, *18*(11), 6711–6718. https://doi.org/10.1128/MCB.18.11.6711

Lau, S. L., & Samman, N. (2006). Recurrence related to treatment modalities of unicystic ameloblastoma: A systematic review. *International Journal of Oral and Maxillofacial Surgery*, *35*(8), 681–690. https://doi.org/10.1016/j.ijom.2006.02.016

Li, N., Sui, J., Liu, H., Zhong, M., Zhang, M., Wang, Y., & Hao, F. (2015). Expression of phosphorylated Akt/mTOR and clinical significance in human ameloblastoma. *International Journal of Clinical and Experimental Medicine*, *8*(4), 5236.

Masthan, K. M. K., Anitha, N., Krupaa, J., & Manikkam, S. (2015). Ameloblastoma. *Journal of Pharmacy & Bioallied Sciences*, *7*(Suppl 1), S167. https://doi.org/10.4103/0975-7406.155891

Mendenhall, W. M., Werning, J. W., Fernandes, R., Malyapa, R. S., & Mendenhall, N. P. (2007). Ameloblastoma. *American Journal of Clinical Oncology*, *30*(6), 645–648. https://doi.org/10.1097/COC.0b013e3181573e59

Micera, A., Lambiase, A., Stampachiacchiere, B., Bonini, S., Bonini, S., & Levi-Schaffer, F. (2007). Nerve growth factor and tissue repair remodeling: TrkANGFR and p75NTR, two receptors one fate. *Cytokine & Growth Factor Reviews*, *18*(3–4), 245–256. https://doi.org/10.1016/j.cytogfr.2007.04.004

Mitsiadis, T. A., & Pagella, P. (2016). Expression of nerve growth factor (NGF), TrkA, and p75NTR in developing human fetal teeth. *Frontiers in Physiology*, *7*, 338. https://doi.org/10.3389/fphys.2016.00338

Mohammad, S., Malkunje, L. R., Singh, N., Das, S., & Mehta, G. (2014). Ameloblastoma of the anterior mandible. *National Journal of Maxillofacial Surgery 5*(1), 47–50. https://doi.org/10.4103/0975-5950.140173

Pagella, P., Catón, J., Meisel, C. T., & Mitsiadis, T. A. (2020). Ameloblastomas exhibit stem cell potential, possess neurotrophic properties, and establish connections with trigeminal neurons. *Cells*, *9*(3), 644. https://www.mdpi.com/2073-4409/9/3/644# https://doi.org/10.3390/cells9030644

Palanisamy, J. C., & Jenzer, A. C. (2019). *Ameloblastoma.*

Patsa, S., Jadav, R. B., Halder, G. C., Ray, J. G., Datta, S., & Deb, T. (2016). Demographic and histopathological variation of ameloblastoma: A hospital-based study. *Journal of Oral and Maxillofacial Pathology: JOMFP*, *20*(2), 230. https://doi.org/10.4103/0973-029X.185937

Reichart, P. A., Philipsen, H. P., & Sonner, S. (1995). Ameloblastoma: Biological profile of 3677 cases. *European Journal of Cancer. Part B, Oral Oncology*, *31B*(2), 86–99. https://doi.org/10.1016/0964-1955(94)00037-5

Settanni, G., Cattaneo, A., & Carloni, P. (2003). Molecular dynamics simulations of the NGF-TrkA domain 5 complex and comparison with biological data. *Biophysical Journal*, *84*(4), 2282–2292. https://doi.org/10.1016/S0006-3495(03)75034-6

Shear, M., & Singh, S. (1978). Age-standardized incidence rates of ameloblastoma and dentigerous cyst on the Witwatersrand, South Africa. *Community Dentistry and Oral Epidemiology*, *6*(4), 195–199. https://doi.org/10.1111/j.1600-0528.1978.tb01149.x

Shivakumar, D., Williams, J., Wu, Y., Damm, W., Shelley, J., & Sherman, W. (2010). Prediction of absolute solvation-free energies using molecular dynamics free energy perturbation and the OPLS force field. *Journal of Chemical Theory and Computation*, *6*(5), 1509–1519. https://doi.org/10.1021/ct900587b

Sodeifian, G., & Razmimanesh, F. (2019). Diffusional interaction behavior of NSAIDs in lipid bilayer membrane using molecular dynamics (MD) simulation: Aspirin and Ibuprofen. *Journal of Biomolecular Structure & Dynamics*, *37*(7), 1666–1684. https://doi.org/10.1080/07391102.2018.1464956

Spiliotopoulos, D., Kastritis, P. L., Melquiond, A. S. J., Bonvin, A. M. J. J., Musco, G., Rocchia, W., & Spitaleri, A. (2016). dMM-PBSA: A new HADDOCK scoring function for protein-peptide docking. *Frontiers in Molecular Biosciences*, *3*, 46. https://doi.org/10.3389/fmolb.2016.00046

Stolf, D. P., Karim, A. C., & Banerjee, A. G. (2007). Genetic aspects of ameloblastoma: A brief review. *Biotechnology and Molecular Biology Reviews*, *2*, 116–122.

Thuckanaickenpalayam Ragunathan, Y., Keniyan Kumar, S., Janardhanam, D., Ravi, A., Santhanam, V., & Ramdas, M. N. (2022). Prevalence and epidemiological profile of ameloblastoma in India: A systematic review and meta-analyses. *Asian Pacific Journal of Cancer Prevention: APJCP*, *23*(11), 3601–3610. https://doi.org/10.31557/APJCP.2022.23.11.3601

Van Der Spoel, D., Lindahl, E., Hess, B., Groenhof, G., Mark, A. E., & Berendsen, H. J. C. (2005). GROMACS: Fast, flexible, and free. *Journal of Computational Chemistry*, *26*(16), 1701–1718. https://doi.org/10.1002/jcc.20291

Vangone, A., Rodrigues, J. P. G. L. M., Xue, L. C., van Zundert, G. C. P., Geng, C., Kurkcuoglu, Z., Nellen, M., Narasimhan, S., Karaca, E., van Dijk, M., Melquiond, A. S. J., Visscher, K. M., Trellet, M., Kastritis, P. L., & Bonvin, A. M. J. J. (2017). Sense and simplicity in HADDOCK scoring: Lessons from CASP-CAPRI round 1. *Proteins*, *85*(3), 417–423. https://doi.org/10.1002/prot.25198

Weng, G., Wang, E., Wang, Z., Liu, H., Zhu, F., Li, D., & Hou, T. (2019). HawkDock: A web server to predict and analyze the protein–protein complex based on computational docking and MM/GBSA. *Nucleic Acids Research*, *47*(W1), W322–W330. https://doi.org/10.1093/nar/gkz397

Wiesmann, C., Ultsch, M. H., Bass, S. H., & de Vos, A. M. (1999). Crystal structure of nerve growth factor in complex with the ligand-binding domain of the TrkA receptor. *Nature*, *401*(6749), 184–188. https://doi.org/10.1038/43705

Yoithapprabhunath, T. R., Renugadevi, S., Ganapathy, N., Dineshshankar, J., Yamunadevi, A., & Nirmal, R. M. (2020). Immunohistochemical detection of nerve growth factor (NGF) in follicular and plexiform ameloblastoma–A novel study. *Journal of Pharmacy & Bioallied Sciences*, *12*(Suppl 1), S569–S575. https://doi.org/10.4103/jpbs.JPBS_185_20

Yuan, T. L., & Cantley, L. (2008). PI3K pathway alterations in cancer: Variations on a theme. *Oncogene*, *27*(41), 5497–5510. https://doi.org/10.1038/onc.2008.245